Print ISSN 2710-0200 *Full text available online at* *Ethiop J Nat Comp Sci.*
Electronic ISSN 2710-0219 *http://journal.uog.edu.et/index.php/EJNCS* *Vol. 4 (2) 586-607*
https://doi.org/*10.20372/ejncs/Ma.2024.019*

ORIGINAL RESEARCH

Mathematical Model for Measles Transmission Control Through age-Structured Vaccination

Saheed A. BELLO[1*], Olumide O OLAIYA[2], Victor A. AKINRINMADE[3] and Kazeem A. ODEYEMI[4]

[1]Training Department, National Water Resources Institutes, Kaduna, Nigeria, Email: kunlebello24@gmail.com,

[2]Mathematical Programme National Mathematical Centre, Sheda, Abuja, Email: oolaiya.o@gmail.com,

[3]Osun State College of Technology, Esa-Oke, Email: akinrinmdevictor@gmail.com

[4]Department of Mathematical Sciences, Osun State University, Osogbo. Email: abidoyekazeem1@gmail.com

[*]Corresponding author: kunlebello24@gmail.com

Received: 9 March 2024/Accepted: 2 July 2024/ Published: 29 August 2024

Abstract

This research presents a mathematical model designed to control measles transmission through age-structured vaccination. Vaccination is pivotal in controlling this contagious disease, and the model investigates various aspects such as existence and uniqueness, minimal recurrence rate, stability analysis of local and global equilibria, and sensitivity analysis. The disease threshold R_0 being a determining factor for persistence of measles $R_0 > 1$ as or it dies out with time as $R_0 < 1$

Utilizing a numerical simulation approach of homotopy perturbation method for numerical analysis, the model assesses the impact of vaccination on the spread of measles whose graphs depicts on each sub-population. Results indicate that vaccination emerges as a potent and efficient control policy, effectively flattening the disease curve and it recommended to policy makers and health practitioners that strict adherence to the use of vaccination to curb the rapid spread of this deadly disease transmission.

Keywords: Measles, Age-Structure, Vaccination, Stability Analysis, Homotopy Perturbation Method

1. Introduction

Measles, a highly contagious viral infection affecting the respiratory system and causing systemic symptoms, presents a challenge to public health globally. To address the pervasive impact of this disease, diverse control strategies have been deployed, with vaccination playing a pivotal role (Kolawole *et al.,* 2020). Vaccination efforts have demonstrated success in curtailing the burden of measles in numerous regions, yet the effectiveness of these initiatives can vary markedly depending on local circumstances and the availability of treatment resources (Kolawole *et al.,* 2020). Undertaking a comprehensive analysis of the efficacy of vaccination as a central component of measles control in settings where treatment resources are already strained. Specifically, we incorporate a saturated treatment function into our examination to capture the intricate relationship between vaccination and treatment amidst limited resources and heightened disease prevalence (Castillo *et al*., 2002). Measles, an infection characterized by fever, cough, runny nose, conjunctivitis, and a distinctive rash, has had a profound impact on human health throughout history (Wusu *et al.,* 2022). This disease, primarily caused by the measles virus, can spread rapidly, leading to severe illness, complications such as pneumonia, encephalitis, and in some cases, fatalities (Kolawole *et al.,* 2022; Mutairu *et al.,* 2022; Mutairu *et al.,* 2023). Over time, various measures have been employed to combat its devastating effects, with vaccination emerging as a crucial intervention in the ongoing battle against measles (Mutairu *et al*., 2023). Control strategies typically encompass a spectrum of interventions, including vaccination campaigns, surveillance, and public health measures, all of which have played a vital role in saving lives and preventing outbreaks (Kolawole *et al.,* 2022). However, the challenge escalates when disease incidence surpasses the capacity of available treatment resources Mutairu et al., 2023; Mutairu et al., 2023; Mutairu et al., 2023; Mutairu et al., 2023; WHO, 2020; Bozkurt *et al.*, 2021). In conditions of high-treatment saturation, the role of vaccination becomes particularly pivotal, as it can alleviate the overall disease burden and alleviate strain on overwhelmed healthcare systems (Kolawole *et al.,* 2020). There is a pressing need to gain deeper insights into the dynamics of vaccination in scenarios where treatment resources are stretched thin (Ferguson *et al.*, 2022; Agusto and Leite, 2019). Through a systematic evaluation of vaccination efficacy in high-treatment saturation conditions, we aim to provide valuable insights that can inform more effective and efficient measles control strategies (Dejong, 2019). The conditions may be prevalent in resource-limited or conflict-affected regions, making our research particularly pertinent to areas where healthcare infrastructure is already under strain (Opoku and Afriyie, 2020; Asamoah, 2018). Measles is transmitted primarily through respiratory droplets and direct contact, with the potential for widespread dissemination in susceptible populations. The consequences of infection can be severe, including complications such as pneumonia, encephalitis, and death (Ayoola *et al.,* 2023). Efforts to control measles have historically relied on a combination of strategies, including vaccination campaigns, early diagnosis, and public health interventions (Ayoola *et al.,* 2022; Castillo *et al.,* 2018). These measures encounter challenges when disease incidence exceeds the healthcare system's treatment capacity. In such scenarios, vaccination emerges as a critical tool for reducing disease burden and preventing outbreaks Bhandari, 2023). This research scrutinizes the effectiveness of vaccination in settings where treatment resources are saturated. By integrating a saturated treatment function, we seek to illuminate the intricate interplay between vaccination and treatment under these demanding circumstances of age-structured base measles disease.

2. Materials and method

2.1. Model formulation

A deterministic mathematical model based on the epidemiological status of population of members that describes the dynamics of measles transmission. The total population N (t) divides into some compartmental classes for a disease-modification as sub-population into susceptible S (t) for children and adult, exposed E (t), infected I (t), and recovered R (t) individuals. The migration/recruitment into the sub-populations that are vulnerable are measured at a rate of A, while transmission of measles is at d. The respective classes are subjected to natural death μ, exposed individuals have disease-induced mortality rate δ. Population of vulnerable individuals are infected at β whose fraction are fats developing in infection at a rate of ρ and infected individuals recover at a rate of γ .The set of individual children that are healed from the disease class through growth/development are converted to adults by m and each proportion of these successively vaccinated individuals are done by birth at v. The model formulation flow therefore depicts is given by fig.1.

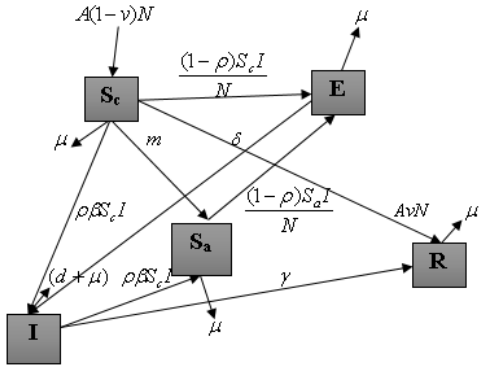

Figure 1. Schematic flow of model description.

$$\frac{dS_c}{dt} = A(1-v)N - \frac{(1-\rho)S_cI}{N} - \rho\beta S_cI - (m + \mu)S_c$$

$$\frac{dS_a}{dt} = mS_c - \frac{(1-\rho)S_aI}{N} - \rho\beta S_aI - \mu S_a \quad (1)$$

$$\frac{dE}{dt} = \frac{(1-\rho)\beta(S_c + S_a)I}{N} - (\delta + \mu)E$$

$$\frac{dI}{dt} = \delta E + \rho\beta(S_c + S_a)I - (\gamma + \mu + d)I$$

$$\frac{dR}{dt} = AvN + \gamma I - \mu R$$

Subject to the following initial conditions

Consider $0 \le v \le 1$ and $0 \le m \le 1$. When $v, m = 0$, susceptible population are not vaccinated as

$$S_c(0) = s_0, S_a = s_0, E(0) = e_0, I(0) = i_0, R(0) = r_0 \ge 0 \quad (2)$$

2.1.1. The existence of the model solution

The parameters of the system (1), which characterizes an epidemic disease in a human population, ought to be nonnegative. Showing that the state variables in the model are nonnegative is crucial to ensuring that the system of differential equations in (1) is well-posed both mathematically and epidemiologically. When the system begins with nonnegative beginning conditions, system (1) is well-posed. $S_c(0) = s_0, S_a(0) = s_0, E(0) = e_0, I(0) = i_0, R(0) = r_0 \ge 0$; In that case, the solutions of system (1) will persist in being nonnegative throughout their evolution, $t > 0$ and that these positive solutions are bounded. We thus apply the following theorems.

Theorem 1

All solutions of system (1) are bounded.

Proof:

Consider the total population

$$N(t) = S_c(t) + S_a(t) + \mathrm{E}(t) + \mathrm{I}(t) + \mathrm{R}(t) \quad (3)$$

The variation in the total population concerning time is given by:

$$\frac{dN(t)}{dt} = \frac{d}{dt}(S_c(t) + S_a(t) + \mathrm{E}(t) + \mathrm{I}(t) + \mathrm{R}(t)) \quad (4)$$

Such that:

$$\frac{dN(t)}{dt} = A - \mu(S + V + E + I + R) - \delta I \Rightarrow$$

$$\frac{dN(t)}{dt} \le A - \mu N \text{at } d = 0$$

Thus, it is obtained that
$\frac{dN(t)}{dt} + \mu N \leq A$, leading to $N(t)e^{\mu t} = \frac{A}{\mu}e^{\mu t} + c$ (5)

Initially,
$N(0) = \frac{A}{\mu} + ce^{-\mu(0)}$, this yields
$c = N(0) - \frac{A}{\mu}$ (6)

Thus, substituting (6) into (5) as time progressively increases yields:
$\lim_{t\to\infty} N(t) \leq \lim_{t\to\infty}\left[\frac{A}{\mu} + \left(N(0) - \frac{A}{\mu}\right)e^{-\mu t}\right] = \frac{A}{\mu}$ (7)

If so $N(0) \leq \frac{A}{\mu}$, then $N(t) \leq \frac{A}{\mu}$. This is a positive invariant set under the flow described by (2) so that no solution path leaves through any boundary $\Re_+^5$. Hence, it is sufficient to consider the dynamics of the model in the domain$\Re_+^5$. In this region the model can be considered has been mathematically and epidemiologically well-posed.
This shows that the total population $N(t)$, and the subpopulation $S(t), E(t), I(t), R(t)$ of the model are bounded and is a unique solution. Hence, its applicability to study physical systems is feasible.

2.1.2. Positivity and boundedness $\Re_+^5$

Theorem 2

Given that the$S_c(0) = s_0 > 0, S_a(0) = s_0 > 0, E(0) = e_0 > 0, I(0) = i_0 > 0, R(0) = r_0 > 0,$ then the solutions $S_c(t), S_a(t), E(t), I(t), R(t)$of the system (1) will always be nonnegative. Consider the compartment of the system of equations for case (1) on the population, as obtained.

Proof:

Let: $\Pi = \left\{(S_c(t), S_a(t), E(t), I(t), R(t)) \in \Re_+^5 : N(t) \leq \frac{A}{\mu}\right\}$ (8)

and $f_i, i = 1,2\ldots.5$where f is a constant.

$$f_1 = A(1-v)N - \frac{(1-\rho)S_c I}{N} - \rho\beta S_c I - (m+\mu)S_c$$
$$f_2 = mS_c - \frac{(1-\rho)S_a I}{N} - \rho\beta S_a I - \mu S_a$$
$$f_3 = \frac{(1-\rho)\beta(S_c + S_a)I}{N} - (\delta+\mu)E$$
$$f_4 = \delta E + \rho\beta(S_c + S_a)I - (\gamma+\mu+d)I$$
$$f_5 = AvN + \gamma I + \mu R\,, \quad (9)$$

Then,
$\left|\frac{\partial f_1}{dS_c}\right| = |(1-\rho) + m + \mu)| < \infty, \left|\frac{\partial f_1}{dS_a}\right| = |0|\,\infty,$
$\left|\frac{\partial f_1}{dE}\right| = |0| < \infty, \left|\frac{\partial f_1}{dI}\right| = |(1-\rho) + \rho\beta| < \infty, \left|\frac{\partial f_1}{dR}\right| = |0| < \infty$

$\left|\frac{\partial f_2}{dS_c}\right| = |m| < \infty, \left|\frac{\partial f_2}{dS_a}\right| = |(1-\rho+\rho\beta+\mu|\,, \left|\frac{\partial f_2}{dE}\right| = |0| < \infty, \left|\frac{\partial f_2}{dI}\right| = |(1-\rho) + \rho\beta| < \infty, \left|\frac{\partial f_2}{dR}\right| = |0| < \infty$

$\left|\frac{\partial f_3}{dS_c}\right| = |(1-\rho)\beta| < \infty, \left|\frac{\partial f_3}{dS_a}\right| = |(1-\rho)\beta|\infty,$
$\left|\frac{\partial f_3}{dE}\right| = |(\delta+\mu)| < \infty, \left|\frac{\partial f_3}{dI}\right| = |(1-\rho)\beta| < \infty, \left|\frac{\partial f_3}{dR}\right| = |0| < \infty$

$\left|\frac{\partial f_4}{dS_c}\right| = |\rho\beta| < \infty, \left|\frac{\partial f_4}{dS_a}\right| = |\rho\beta| < \infty, \left|\frac{\partial f_4}{dE}\right| = |\delta| < \infty,$
$\left|\frac{\partial f_4}{dI}\right| = |\rho\beta + (d+\mu+\gamma)| < \infty, \left|\frac{\partial f_4}{dR}\right| = |0| < \infty$

$\left|\frac{\partial f_5}{dS_c}\right| = |0| < \infty, \left|\frac{\partial f_5}{dS_a}\right| = |0| < \infty, \left|\frac{\partial f_5}{dE}\right| = |0| < \infty,$
$\left|\frac{\partial f_5}{dI}\right| = |\gamma| < \infty, \left|\frac{\partial f_5}{dR}\right| = |\mu| < \infty$ (10)

Equation (10) demonstrates the presence of system (1) within the positive quadrant, leading it to ultimately enter and persist in the attracting subset Π. Consequently, the set comprises both the local and global attractors of system (1). As a result, the set is characterized as compact, positively invariant, and attractively influential with respect to the system. The solution of the model is bounded, well-posed and epidemiologically and mathematical represented.

2.1.3. Measles-non-Infected Equilibrium State

The measles-non-infected equilibrium state represents a scenario in which the system is entirely free from the contagious disease. Consequently, when the number of infected individuals (I), it follows that the numbers of exposed (E) and recovered (R), i.e. $I = E = 0$. In

this context, the solution for the measles-free equilibrium point can be derived as follows:

$$\frac{dS_c}{dt} = \frac{dS_a}{dt} = \frac{dE}{dt} = \frac{dI}{dt} = \frac{dR}{dt} = 0 \qquad (11)$$

$$A(1-v)N - \frac{(1-\rho)S_c I}{N} - \rho\beta S_c I - (m+\mu)S_c = 0$$

$$mS_c - \frac{(1-\rho)S_a I}{N} - \rho\beta S_a I - \mu S_a = 0$$

$$\frac{(1-\rho)\beta(S_c+S_a)I}{N} - (\delta+\mu)E = 0$$

$$\delta E + \rho\beta(S_c+S_a)I - (\gamma+\mu+d)I = 0$$

$$AvN + \gamma I + \mu R = 0 \qquad (12)$$

At no outbreak of measles the disease class subjected as $t = 0$, from (12),

$AvN + \gamma I + \mu R = 0, R = \frac{AvN}{\mu}$. Similarly,

$S_c = \frac{AN(1-v)}{(m+\mu)}$where $S_a = \frac{m[A(1-v)N]}{\mu(m+\mu)}$

Thus, the disease-free equilibrium yields: $(S_c, S_a, E, I, R) = \left(S_c = \frac{AN(1-v)}{(m+\mu)}, S_a = \frac{m[A(1-v)N]}{\mu(m+\mu)}, E_0 = 0, I_0 = 0, R_0 = \frac{AvN}{\mu}\right)$ (13)

2.1.4. Steady-State Prevalence

Measles prevalence on (S_c, S_a, E, I, R) at $t \neq 0$, highlighting its dynamic nature.to measure vital role on its outbreaks and protect the population. Let $E_e = (S_c^*, S_a^*, E^*, I^*, R^*)$ at steady state $I \neq 0$. Consider the system of equation in (1) the equilibrium points are:

$$S_c^* = \frac{A(1-v)\mu^2\sqrt{(1-v)(d+\gamma+\mu)v(\mu+\gamma+\delta)}\beta vN(1-v)^2[AvN+(\mu+\gamma+\delta)\beta^*]+v[A(\mu+\gamma+\delta)Av\gamma\beta_i+\delta)]}{\mu(d+\mu)[(\mu+\gamma+\delta)(\mu+\gamma+\delta)+(1-v)]}$$

$$S_a^* = \frac{A(1-v)N\beta(\beta A(N-1)\rho + \mu^2 + (\gamma+d)\mu + (N\rho+\mu(d+\gamma+\mu))}{\mu\beta A(\mu+\gamma+\delta)[\sqrt{(1-v)(d+\mu)}(\mu+\gamma+\delta)+(1-\varepsilon)]},$$

$$E^* = \frac{\beta\eta A(1-\varepsilon) + \rho v(\delta+\gamma+\mu)^2}{\rho\beta A\sqrt{(d+v+\mu)(\delta+\mu)} + (1-v)\rho v\beta A}$$

$$I^* = \frac{(1-v)][Av\beta(d+\mu)+(\mu+\gamma+\delta)\rho^2]}{[\mu^2(d+\mu)+(1-v)]} - \frac{\sqrt{(d+\mu+\delta)(\delta+\mu)}}{(1-v)^{-1}(\gamma+\mu+\delta)A\rho} \qquad (14)$$

$$R^* = (1-v)^{-1}\sqrt{\frac{[(\gamma+\mu+\delta)\sigma\gamma+d]A^2\beta v+\rho v^2}{(d+\mu+\delta)(\gamma+\mu+\delta)(d+\mu+\delta)}}$$

2.1.5. The disease threshold R_*

The disease threshold/basic reproduction number, denoted as R_*, measures the potential for new measles infections from a single carrier or infected individual in a population with no prior infections. To determine the system (1), we apply the next-generation method, focusing on the infectious classes E and I. This involves calculating the F and V matrices, representing the rates of new infections and transitions into and out of the infected compartment, respectively. From the equations in the system (1), we derive these matrices as follows. $R_* = \rho(M - \lambda I)$ where $M = F \times V^{-1}$and ρ is the spectral radius of the matrix $|G - \lambda I|$.

From the system of equation (1) it is obtained for matrix $F$and V:

$$F_i = \left(\frac{\partial f_i(x_i)}{\partial x_j}\right), V_i = \left(\frac{\partial v_i(x_i)}{\partial x_j}\right) \qquad (15)$$

Such that

$$f = \begin{pmatrix} (1-\rho)\beta(S_c + S_a) \\ 0 \end{pmatrix} \text{ And } v = \begin{pmatrix} (\delta+\mu)E \\ -\delta E - [\rho\beta(S_c+S_a) + (\gamma+\mu+d)]I \end{pmatrix} \quad (16)$$

Then,

$$F = \begin{pmatrix} 0 & \frac{(1-\rho)\beta(S_c+S_a)}{N} \\ 0 & 0 \end{pmatrix} V = \begin{pmatrix} (\delta+\mu) & 0 \\ -\delta & \rho\beta(S_c+S_a) + (\gamma+\mu+d) \end{pmatrix}$$

$$V^{-1} = \begin{pmatrix} \frac{(d+\mu+\gamma)-\rho\beta(S_c+S_a)}{(d+\mu+\gamma)(d+\mu)-\rho\beta(S_c+S_a)} & \frac{\delta}{(d+\mu+\gamma)(d+\mu)-\rho\beta(S_c+S_a)} \\ 0 & \frac{(d+\mu)}{(d+\mu+\gamma)(d+\mu)-\rho\beta(S_c+S_a)} \end{pmatrix} \quad (17)$$

Thus, the R_* is obtained as:

$$R_* = \begin{pmatrix} 0 & \frac{(1-\rho)\beta(S_c+S_a)}{N} \\ 0 & 0 \end{pmatrix} \begin{pmatrix} \frac{(d+\mu+\gamma)-\rho\beta(S_c+S_a)}{(d+\mu+\gamma)(d+\mu)-\rho\beta(S_c+S_a)} & \frac{\delta}{(d+\mu+\gamma)(d+\mu)-\rho\beta(S_c+S_a)} \\ 0 & \frac{(d+\mu)}{(d+\mu+\gamma)(d+\mu)-\rho\beta(S_c+S_a)} \end{pmatrix}$$

$$R_* = \frac{\beta(1-\rho)A((1-v)N)\delta}{(\delta+\mu)[(\mu d+\mu^2+\mu\gamma)-\rho\beta(A(1-v)N]} \quad (18)$$

2.1.6. Quantitative Analysis of R_ε

Here, we conduct a quantitative analysis of R_ε to assess its metric progression concerning each intervention method. By excluding the values of intervention parameters, we asses equation (18) using the baseline values provided in Table 1, yielding equation (18), subsequently resulting in equations (19) through (23). The outcomes of these calculations are presented in Table 2.

$$R_\varepsilon = \frac{0.1(1\text{-}\rho)(0.542(0.018+v)\rho_1+0.056+(0.42)(1\text{-}v)\beta\text{-}0.09d)}{(0.024+0.018\rho)(0.056+0.03\tau))} \quad (19)$$

$$R_\varepsilon = f(\rho_1)|_{\substack{\gamma=0 \\ v=0 \\ \rho=0}} = \text{-}1.3097\gamma+1.486 \quad (20)$$

$$R_\varepsilon = f(\tau)|_{\substack{v=0 \\ \rho_1=0 \\ A=0}} = \frac{0.0057}{0.021A+0.0856} \quad (21)$$

$$R_\varepsilon = f(\rho_2)|_{\substack{c=0 \\ \rho_1=0 \\ \tau=0}} = \frac{0.077(0.06+0.51\rho_2)}{0.925+0.92\mu} \quad (22)$$

$$R_\varepsilon = f(c)|_{\substack{v=0 \\ \tau=0 \\ \rho=0}} = 1.337\delta\text{-}1.46\text{v} \quad (23)$$

Table II: standalone metric of vaccination and general awareness on R_ε

	A					B					C				
s/n	ρ	A	δ	d	R_ε	ρ	A	δ	d	R_ε	ρ	A	δ	d	R_ε
1	0	0	0	0	1.45938	0	0	0	0	1.45915	0	0	0	0	1.45916
2	0.2	0	0	0	1.37330	0	0.2	0	0	1.16741	0	0	0.2	0	0.25432
3	0.4	0	0	0	0.93382	0	0.4	0	0	0.87542	0	0	0.4	0	0.202468
4	0.6	0	0	0	0.67123	0	0.6	0	0	0.58375	0	0	0.6	0	0.184168
5	0.8	0	0	0	0.40856	0	0.8	0	0	0.29187	0	0	0.8	0	0.174811
6	1.0	0	0	0	0.14591	0	1.0	0	0	0.29101	0	0	1.0	0	0.169130

Table III: standalone metric of therapy efficacy and combine metric of all interventions on R_ε

	A						B					
s/n	ρ	A	δ	d	R_ε		**s/n**	ρ	A	δ	d	R_ε
1	0	0	0	0	1.3635		1	0	0	0	0	1.47265
2	0	0	0	0.2	1.9484		2	0.2	0.2	0.2	0.2	1.36305
3	0	0	0	0.4	0.4763		3	0.4	0.4	0.4	0.4	0.98381
4	0	0	0	0.6	0.6723		4	0.6	0.6	0.6	0.6	0.09836
5	0	0	0	0.8	0.4484		5	0.8	0.8	0.8	0.8	0.73639
6	0	0	0	1.0	0.1441		6	1	1	1	1	0.93411

2.1.7. Asymptotic stability of the disease-free state

This section examines the stability of the disease-free state for measles by analyzing the basic reproduction number's impact. When the reproduction number is $R_* < 1$, the disease declines, and we determine stability using a Jacobian matrix and a characteristic equation.

Theorem 3

The disease-free state of the model is locally asymptotically Stable $R_* < 1$ meanwhile it is unstable if the basic reproduction $R_* > 1$.

Proof:

Consider that the disease-free equilibrium is obtained as the Jacobian matrix of the system of (1) is obtained and evaluated at the disease free-state using the linearization method obtaining that $|J_E - \lambda I| = 0$. The resulting matrix from the compartments of the model formulation is obtained from respective derivatives of the state parameters as:

$$J_{(E_1)} = \begin{pmatrix} -(m+\mu) & 0 & 0 & -\left[\frac{(1-\rho)\beta AN(1-v)}{N(m+\mu)} + \frac{\rho\beta ANm(1-v)}{\mu(m+\mu)}\right] & 0 \\ m & -\mu & 0 & \left[\frac{(1-\rho)mAN(1-v)}{N\mu(m+\mu)} + \frac{\beta AN(1-v)}{N(m+\mu)}\right] & 0 \\ 0 & 0 & -(\delta+\mu) & \left[\frac{\rho\beta AN(1-v)}{(m+\mu)} + \frac{ANm(1-v)}{\mu(m+\mu)}\right] & 0 \\ 0 & 0 & \delta & -(d+\mu+\gamma) & 0 \\ 0 & 0 & 0 & \gamma & -\mu \end{pmatrix} \quad (24)$$

Computing for the eigenvalues, $|J_{E_1} - \lambda_i I| = 0$ for each respective $\lambda_i, i = 1\ldots5$

$$\begin{vmatrix} -(m+\mu)-\lambda & 0 & 0 & -\left[\frac{(1-\rho)\beta AN(1-v)}{N(m+\mu)} + \frac{\rho\beta ANm(1-v)}{\mu(m+\mu)}\right] & 0 \\ m & -\mu-\lambda & 0 & \left[\frac{(1-\rho)mAN(1-v)}{N\mu(m+\mu)} + \frac{\beta AN(1-v)}{N(m+\mu)}\right] & 0 \\ 0 & 0 & -(\delta+\mu)-\lambda & \left[\frac{\rho\beta AN(1-v)}{(m+\mu)} + \frac{ANm(1-v)}{\mu(m+\mu)}\right] & 0 \\ 0 & 0 & \delta & -(d+\mu+\gamma)-\lambda & 0 \\ 0 & 0 & 0 & \gamma & -\mu-\lambda \end{vmatrix} = 0$$

as obtained:

$$\left.\begin{aligned} &\lambda_1 = -(m+\mu), \lambda = -\mu, \lambda = -(d+\mu+\gamma), \begin{vmatrix} -(\delta+\mu) & \left[\frac{\rho\beta AN(1-v)}{(m+\mu)} + \frac{ANm(1-v)}{\mu(m+\mu)}\right] \\ \delta & (d+\mu+\gamma) \end{vmatrix}, \lambda_3 = -\left[\frac{\rho\beta AN(1-v)}{(m+\mu)} + \frac{ANm(1-v)}{\mu(m+\mu)}\right], \\ &\lambda_4 = -(\delta+\mu) \end{aligned}\right\} \quad (25)$$

The eigenvalues are negatively invariant in the region $\Re_+^5$ for each $\lambda_i < 0$ are hence the system of (20) is locally asymptotically stable.

2.1.8. Regional Resilience of the Persistent

Equilibrium

Theorem 4

The regional resilience of the persistent equilibrium of the model is locally asymptotically stable whenever $R_* < 1$ and unstable respectively when each of its eigenvalues of the matrix is $\lambda > 0$.

Proof:

Suppose, $S_c = x + S_c^*, S_a = y + S_a^*, E = z + E^*, I = p + I^*, R = q + R^*$
Linearizing equation (1), is then obtained as

$$\left.\begin{aligned} \frac{dx}{dt} &= -(1-\rho)\beta xp - \rho\beta xp - (m-\mu)x + \text{higher order } + \text{ nonlinear terms...} \\ \frac{dy}{dt} &= mx - (1-\rho)\beta yp - \rho\beta yp - \mu y + \text{higher order } + \text{ nonlinear terms...} \\ \frac{dz}{dt} &= (1-\rho)\beta xp + yp - (\delta+\mu)z + \text{higher order } + \text{ nonlinear terms...} \\ \frac{dp}{dt} &= \delta z + \rho\beta(x+y)p - (d+\mu+\gamma)p + \text{higher order } + \text{ nonlinear terms...} \\ \frac{dq}{dt} &= \gamma p - \mu q + \text{Higher order } + \text{ nonlinear terms...} \end{aligned}\right\} \quad (26)$$

Jacobian matrix of the system of (26),

$$\begin{pmatrix} -\left[\frac{\rho\beta AmN(1-v)}{\mu(m+\mu)}\right] & 0 & 0 & -\frac{(1-\rho)\beta S_c}{N}+\rho S_c & 0 \\ m & -\left[\frac{(1-\rho)\beta S_c}{N}+\rho S_c+I\mu\right] & 0 & \frac{(1-\rho)\beta S_a}{N}+\rho S_a & 0 \\ (1-\rho)\frac{\beta I}{N} & (1-\rho)\frac{\beta I}{N} & -(\delta+\mu) & \frac{(1-\rho)\beta S_c}{N}+\frac{\beta S_a}{N} & 0 \\ \rho\beta I & \rho\beta & \delta & -[(d+\mu+\gamma)-\rho\beta(S_a+S_c)] & 0 \\ 0 & 0 & 0 & \gamma & -\mu \end{pmatrix} \quad (27)$$

$$\begin{pmatrix} -[(1-2\rho\beta p-m-\mu)] & 0 & 0 & -2\rho\beta & 0 \\ m & -[(1-2\rho\beta p-\mu)] & 0 & 2\rho\beta & 0 \\ (1-\rho)\beta p & p & -(\delta+\mu) & 0 & 0 \\ \rho\beta & \rho\beta p & \delta & -[(d+\mu+\gamma)-\rho\beta(x+y)] & 0 \\ 0 & 0 & 0 & \gamma & -\mu \end{pmatrix}$$

The resulting eigenvalue of the above matrix is obtained as:

$$\left([\tfrac{\rho\beta AmN(1-v)}{\mu(m+\mu)}]+[\tfrac{(1-\rho)\beta S_c}{N}+\rho\beta+\mu]+(\delta+\mu)+(d+\mu+\gamma)-\rho\beta(S_c+S_a)]+\mu\right) \quad (28)$$

The trace of $J(E_e)<0$. Thus, the Jacobian matrix $J(E_e)$ has eigenvalues that contains negative root parts. Therefore, we conclude that the endemic equilibrium point is locally asymptotically stable. Hence, the persistent resilience of the model in a region are asymptotically stable.

2.1.9. Global stability of disease-free equilibrium

We employ Lyapunov's function approach, to establish the global asymptotic stability of the model solution for equation (1) at the disease-free equilibrium, utilizing the Lyapunov algorithm

$$\Phi(t,S_c,S_a,E,I,R)=C_1I_1+C_2I_2 \quad (29)$$

$$\frac{d\Phi}{dt}=C_1I_1^{\bullet}+C_2I_2^{\bullet}=C_1\left(\frac{(1-\rho)\beta(S_cI_2+S_aI_2)}{N}-(\delta+\mu)I_1\right)+C_2(\delta I_1+\rho\beta(S_cI_2+S_aI_2)-(d+\gamma+\mu)I_2)$$

$$=C_1\frac{(1-\rho)\beta S_cI_2}{N}+C_1\frac{(1-\rho)\beta S_aI_2}{N}-C_1(\delta+\mu)I_1+C_2\delta I_1+C_2\rho\beta(S_cI_2+S_aI_2)-C_2(d+\gamma+\mu)I_2$$

$$\leq C_1\left(\frac{(1-\rho)\beta S_cI_2}{N}+\frac{(1-\rho)\beta S_aI_2}{N}-(\delta+\mu)\right)I_1+C_2(\delta I_1+\rho\beta(S_cI_2+S_aI_2)-(d+\gamma+\mu))I_2$$

$$S_0=\frac{\pi N(1-\varepsilon)}{((1-\varepsilon)(\lambda+v+\mu)+\omega)},V_0=\frac{\pi N}{((\varepsilon-1)(\lambda+v+\mu)+\omega)},C_1=\frac{(\sigma+\mu+\gamma_c)}{(\sigma+\mu+\gamma_c)},C_2$$

$$=\left(\frac{(\gamma_i+\mu+\delta)(1+\alpha)}{\tau(\gamma_i+\mu+\delta)(1+\alpha)}\right)$$

$$\frac{d\Phi}{dt} \leq C_1\left(\frac{\pi\tau(\alpha+1)(1-\varepsilon)+\sqrt{\pi\eta(1-\varepsilon)\beta+(\omega\kappa+\nu+\mu)}}{((1-\varepsilon)^2\alpha(\lambda+\nu+\mu)+\tau\omega)(\sigma+\gamma_e+\mu)(\delta+\gamma_i+\mu)}-\frac{(\sigma+\mu+\gamma_c)}{(\sigma+\mu+\gamma_c)}\right)I$$
$$-C_2\left(\left(\frac{(\gamma_i+\mu+\delta)(1+\alpha)}{\tau(\gamma_i+\mu+\delta)(1+\alpha)}\right)-\left(\frac{(\gamma_i+\mu+\delta)(1+\alpha)}{\tau(\gamma_i+\mu+\delta)(1+\alpha)}\right)\right)$$
$$\frac{d\Phi}{dt} \leq \psi(R_0-1) \qquad (30)$$

It is pertinent to note that when at $t \to \infty$and $C_1 < 1$. Substituting into the model system of equation (18) reveals that, based on LaSalle's invariance principle $\frac{d\Phi}{dt} = 0$, is globally asymptotically stable whenever $R_* > 1$

2.1.10. Global stability for endemic equilibrium

Theorem 5

The model system of equation (1) has no periodic orbits.

Proof:

We employ the concept of Dulac's criterion. Let $X = (S, I, H, R, P)$ define the Dulac's function $G = \frac{1}{SI}$. The following system of equations are obtained;

$$G\frac{dS_c}{dt} = \frac{1}{SI}\left\{A(1-v)N - \frac{(1-\rho)S_cI}{N} - \rho\beta S_cI - (m+\mu)S_c\right\}$$

$$G\frac{dS_a}{dt} = \frac{1}{SI}\left\{mS_c - \frac{(1-\rho)S_aI}{N} - \rho\beta S_aI - \mu S_a\right\}$$

$$G\frac{dE}{dt} = \frac{1}{SI}\left\{\frac{(1-\rho)\beta(S_c+S_a)I}{N} - (\delta+\mu)E\right\} \qquad (31)$$

$$G\frac{dI}{dt} = \frac{1}{SI}\{\delta E + \rho\beta(S_c+S_a)I - (\gamma+\mu+d)I\}$$

$$G\frac{dR}{dt} = \frac{1}{SI}\{AvN + \gamma I - \mu R\}$$

The above system of equations results to:

$$G\frac{dS_c}{dt} = \left\{\frac{A(1-v)N}{SI} - [(1-\rho)+\rho\beta] - \frac{(m+\mu)}{I}\right\}$$

$$G\frac{dS_a}{dt} = \left\{\frac{m}{I} - \frac{(1-\rho)}{N} - \rho\beta - \frac{\mu}{I}\right\}$$

$$G\frac{dE}{dt} = \left\{\frac{(1-\rho)\beta}{N} - \frac{(\delta+\mu)E}{SI}\right\} \qquad (32)$$

$$G\frac{dI}{dt}=\left\{\frac{\delta E}{SI}+\rho\beta-\frac{(\gamma+\mu+d)}{S}\right\}$$

$$G\frac{dR}{dt}=\left\{\frac{AvN}{SI}+\frac{\gamma}{S}-\frac{\mu R}{SI}\right\}$$

At $t>0$ orbital resolution of the system of equations is given by $\frac{d(GX)}{dt}$ as obtained below.

$$\frac{d(GX)}{dt}=\frac{\partial}{\partial S_c}\left\{G\frac{dS_c}{dt}\right\}+\frac{\partial}{\partial S_a}\left\{G\frac{dS_a}{dt}\right\}+\frac{\partial}{\partial E}\left\{G\frac{dE}{dt}\right\}+\frac{\partial}{\partial I}\left\{G\frac{dI}{dt}\right\}+\frac{\partial}{\partial R}\left\{G\frac{dR}{dt}\right\}$$

$$\frac{d(GX)}{dt}=\frac{\partial}{\partial S_c}\left\{\frac{A(1-v)N}{SI}-[(1-\rho)+\rho\beta]-\frac{(m+\mu)}{I}\right\}+\frac{\partial}{\partial S_a}\left\{\frac{m}{I}-\frac{(1-\rho)}{N}-\rho\beta-\frac{\mu}{I}\right\}$$
$$+\frac{\partial}{\partial E}<0\left\{\frac{(1-\rho)\beta}{N}-\frac{(\delta+\mu)E}{SI}\right\}+\frac{\partial}{\partial I}\left\{\frac{\delta E}{SI}+\rho\beta-\frac{(\gamma+\mu+d)}{S}\right\}+\frac{\partial}{\partial R}\left\{\frac{AvN}{SI}+\frac{\gamma}{S}-\frac{\mu R}{SI}\right\}$$

$$\frac{d(GX)}{dt}=\left\{-\frac{A(1-v)+[(1-\rho)+\rho\beta]+(m+\mu)}{SI}\right\}+\left\{-\frac{m+(1-\rho)-(\rho\beta+\mu)}{I}\right\}$$
$$+\left\{-\frac{(1-\rho)\beta+((\delta+\mu))}{I}\right\}+\left\{-\frac{\delta+\rho\beta+(\gamma+\mu+d)}{SI}\right\}+\left\{-\frac{Av+\gamma-\mu}{SI}\right\} \quad (33)$$

$$\frac{d(GX)}{dt}=-\left\{\begin{matrix}\frac{A(1-v)+[(1-\rho)+\rho\beta]+(m+\mu)}{SI}+\frac{m+(1-\rho)-(\rho\beta+\mu)}{I}\\+\frac{(1-\rho)\beta+(\delta+\mu)}{I}+\frac{\delta+\rho\beta+((\gamma+\mu+d))}{SI}+\frac{Av+\gamma-\mu}{SI}\end{matrix}\right\} \quad (34)$$

$$\frac{d(GX)}{dt}=-\left\{\frac{\begin{matrix}A(1-v)+[(1-\rho)+\rho\beta]+\sigma(m+\mu)+\gamma[m+m(1-\rho)-\\v(\rho\beta+\mu)]+(1-\rho)\beta+(\delta+\mu)\end{matrix}}{SI}\right\}<0$$

This implies that the system has no closed orbit. It therefore portray epidemiologically that, no existence of a periodic orbit which implies that there are fluctuations in the number of infective, which makes it pretty obvious that in allocation of resources for the control of the disease, vaccination will help to eradicate the rapid spread of measles with time.

3. Sensitivity analysis of R_*

The primary aim is to assess the sensitivity of the basic reproduction number, by computing its derivative concerning all relevant parameters. This analysis will result in the determination of the normalized forward sensitivity index, denoted

$$R_*=\frac{\beta(1-\rho)A((1-v)N)\delta}{(\delta+\mu)[(\mu d+\mu^2+\mu\gamma)-\rho\beta(A(1-v)N]}$$

$$\frac{\partial R_*}{\partial\beta}=\frac{\partial R_*}{\partial\beta}\times\frac{\beta}{R_*}=0.01206000$$

$$\frac{\partial R_0}{\partial d}=\frac{\partial R_0}{\partial d}\times\frac{d}{R_0}=0.00130200$$

$$\frac{\partial R_*}{\partial\rho}=\frac{\partial R_*}{\partial\rho}\times\frac{\rho}{R_*}=1.03267370$$

$$\frac{\partial R_*}{\partial\gamma}=\frac{\partial R_*}{\partial\gamma}\times\frac{\gamma}{R_*}=0.00130200 \quad (35)$$

$$\frac{\partial R_*}{\partial A} = \frac{\partial R_*}{\partial A} \times \frac{A}{R_*} = 0.18743076$$

$$\frac{\partial R_*}{\partial \mu} = \frac{\partial R_*}{\partial \mu} \times \frac{\mu}{R_*} = 0.15356728$$

$$\frac{\partial R_*}{\partial v} = \frac{\partial R_*}{\partial v} \times \frac{v}{R_*} = 0.00001001$$

$$\frac{\partial R_*}{\partial N} = \frac{\partial R_*}{\partial N} \times \frac{N}{R_*} = 1.00000000$$

$$\frac{\partial R_*}{\partial \delta} = \frac{\partial R_*}{\partial \delta} \times \frac{\delta}{R_*} = 0.00000040$$

Table 1. Sensitivity analysis and parameter indices

Parameters	Sensitivity indices
β	0.01206000
σ	1.03267370
α	0.18743076
κ	0.00001001
δ	1.00000000
ω	1.000201001

Table 1 shows that the sensitivity indices of are positively invariant in $\Re_5^+$ the sensitivity indices depend on the values of the each parameters of R_*, and this brings about changes in the values that will affect the the behaviour of the threshold on the spread or vanity of measles disease. Based on the table, we can conclude that parameters are the most sensitive to the basic reproduction number in equation (18) of the measles model. Particularly, increasing the value of σ will result in a 96.96% increase inR_*, while increasing the value of k will lead to a 91.52% decrease in R_*.

3.1 Numerical simulation

Homotopy Perturbation Method (HPM) is an elegant and powerful method to solve linear and non-linear partial differential equations. As we know to get an exact solution of non- linear partial differential equation is very difficult, so any kind of perturbative approach is acceptable depending on its criteria. HPM provides an analytical solution by using the initial conditions. It is interesting to note that only a few terms are required to obtain a most accurate approximate solution.

In this section, we have illustrated the basic idea of homotopy perturbation method to apply in non-linear equations. Let us consider the following non-linear differential equation of the form.

$$A(u) - f(r) = 0, r \in \Omega \qquad (36)$$

Subject to the boundary conditions:

$$B = \left(u, \frac{\partial u}{\partial n}\right) = 0, r \in \Gamma, \qquad (37)$$

Where A is a general differential operator, B is a boundary operator, f(r) a known analytical function and Γ is the boundary of the domain Ω. In general one can divide the operation A into two parts: Linear and non-linear. That means

$$A = L + N$$

Where L is Linear and N is the non-linear,
Hence, equation (3) can now be rewritten as

$$L(u) + N(u) + f(r) = 0, r \in \Omega \qquad (38)$$

By the homotopy technique, one can construct a homotopy in the following way

$$v(r, p): \Omega \times [0,1] \to R$$

This satisfies

$$H(V, P) = (1 - P)[L(v) - L(u_0)] + P[A(v) - f(r) = 0, P \in [0,1], r \in \Omega \qquad (39)$$

Constructing a Homotopy perturbation method using an algorithm developed on each compartment of the model. We conduct the numerical simulation on the mathematical model using the concept of homotopy perturbation method which brings about creating the following correctional scheme for the model equation.

Table 2. Description of parameters, values, and reference

Variable	*Description*		
$S_c(t)$	Susceptible (Vulnerable Children) population		
$S_a(t)$	Susceptible (Vulnerable Adulthood) population		
E(t)	Exposed population		
I(t)	Infected population		
R(t)	Recovered population		
Parameter	**Description**	**Values**	**References**
N	Total population	0.002	(Mutairu *et al.*, 2023)
m	Conversion rate of susceptible children to adult group	0.001	(Mutairu *et al.*, 2023)
v	The proportion of those successively vaccinated at birth	0.5	(Kolawole *et al.*, 2020)
ρ	Fraction of fast-developing infection cases	0.2	(Mutairu *et al.*, 2023)
γ	Rate of recovery after being infected	0.03	(Kolawole *et al.*, 2020)
μ	Natural death	1.0	(Wusu *et al.*, 2022)
δ	Disease induced death	0.0016	(Asamoah, 2018)
A	Recruitment rate	0.113	(Kolawole *et al.*, 2023)
β	infected rate	1.0126	(Bozkurt *et al.*, 2021)
d	Rate of transmission	0.33182	(Kolawole *et al.*, 2020)

$$(1-p)\frac{dS_c}{dt} + p\left(\frac{dS_c}{dt} - [A(1-v)N - \frac{(1-\rho)S_cI}{N} - \rho\beta S_cI - (m+\mu)S_c]\right) = 0$$

$$(1-p)\frac{dS_a}{dt} + p\left(\frac{dS_a}{dt} - [mS_c - \frac{(1-\rho)S_aI}{N} - \rho\beta S_aI - \mu S_a]\right) = 0$$

$$(1-p)\tfrac{dE}{dt} + p\left(\tfrac{dE}{dt} - [\tfrac{(1-\rho)\beta(S_c+S_a)I}{N} - (\delta+\mu)E)E]\right) \quad (40)$$

$$(1-p)\frac{dI}{dt} + p\left(\frac{dC}{dt} - [\delta E + \rho\beta(S_c + S_a)I - (\gamma+\mu+d)I]\right) = 0$$

$$(1-p)\frac{dR}{dt} + p\left(\frac{dR}{dt} - [AvN + \gamma I - \mu R]\right) = 0$$

The following correctional series are assumed as solutions for (1) such that

$$S_c(t) = \sum_{k=0}^{n} p^k s_k(t), S_a(t) = \sum_{k=0}^{n} p^k v_k(t), E(t) = \sum_{k=0}^{n} p^k e_k(t),$$
$$I(t) = \textstyle\sum_{k=0}^{n} p^k i_k(t), R(t) = \sum_{k=0}^{n} p^k r_k(t), \quad (41)$$

This series converges as p tends to in each of the iterations is subjected to the initial conditions as $t \to 1$. Evaluating (32) and comparing coefficients of p^n yields the following at $n = 1$

$$\frac{dS_o}{dt} = 0, \frac{dS_o}{dt} = 0, \frac{dE_o}{dt} = 0, \frac{dI_o}{dt} = 0, \frac{dR_o}{dt} = 0 \tag{42}$$

Solving these equations using the initial constraints
$S_0(t) = s_0, S_0(t) = e_0, E_0(t) = e_0, I_0(t) = i_0, R_0(t) = r_0$, at this initial condition, the result obtained from (32) is deduced as

$$\begin{aligned} S_{c1}(t) &= (\pi + mv + \kappa r_0 - \gamma s_0 - (v + \mu)s_0)t \\ S_{a1}(t) &= (-\beta_1 s_0 - \beta_2 v_0 + \mu v_0)t \\ E_1(t) &= (\alpha s_0 i_0 - \mu e_0 - \sigma e_0)t \\ I_1(t) &= (\sigma e_0 - \mu i_0 - \delta i_0 - \rho i_0)t \\ R_1(t) &= (\rho i_0 - \mu r_0)t \end{aligned} \tag{43}$$

The successive iterations of the results obtained at $n = 2$ yields

$$s_2(t) = \frac{1}{2}t^2\begin{pmatrix} \alpha^3 {i^2}_0 s_0 + \alpha^2 \mu i_0 s_0 + \alpha^2 \beta_1 i_0 s_0 - \alpha^2 \beta_2 i_0 v_0 - \alpha^2 \theta i_0 + \alpha\delta i_0 s_0 + \\ 2\alpha\mu i_0 s_0 + \alpha\rho_0 s_0 - \alpha\sigma e_0 s_0 + \alpha\beta_{1_0} s_0 + \mu^2 s_0 + 2\mu\beta_1 s_0 - 2\mu\beta_1 v_0 - \\ {\beta_1}^2 s_0 + \beta_2\beta_1 s_0 - \beta_2\beta_1 v_0 - {\beta_2}^2 v_0 - \mu\theta - \theta\beta_1 \end{pmatrix}$$

$$s_{2a}(t) = \frac{1}{2}t^2\begin{pmatrix} \alpha^3 {i^2}_0 s_0 + \alpha^2 \mu i_0 s_0 + \alpha^2 \beta_1 i_0 s_0 - \alpha^2 \beta_2 i_0 v_0 - \alpha^2 \theta i_0 + \\ \alpha\delta i_0 s_0 + 2\alpha\mu i_0 s_0 + \alpha\rho_0 s_0 - \alpha\sigma e_0 s_0 + \alpha\beta_{1_0} s_0 + \mu^2 s_0 \\ +2\mu\beta_1 s_0 - 2\mu\beta_1 v_0 - {\beta_1}^2 s_0 + \beta_2\beta_1 s_0 - \beta_2\beta_1 v_0 - {\beta_2}^2 v_0 - \mu\theta - \theta\beta_1 \end{pmatrix}$$

$$e_2(t) = -\frac{1}{2}t^2\begin{pmatrix} \alpha^2 {i_0}^2 s_0 + \alpha\delta i_0 s_0 + 3\alpha\mu i_0 s_0 + \alpha\rho_0 s_0 - \alpha\sigma e_0 s_0 + \alpha\sigma_{1_0} s_0 + \alpha\beta_1 i_0 s_0 \\ -\alpha\beta_2 i_0 v_0 - \alpha\theta i_0 - \mu^2 e_0 - 2\mu\sigma e_0 - \sigma^2 e_0 \end{pmatrix}$$

$$I_2(t) = -\tfrac{1}{2}t^2\begin{pmatrix} \alpha\beta_1 i_0 s_0 - \mu^2 v_0 + 2\mu\beta_1 s_0 - 2\mu\beta_2 v_0 + {\beta_1}^2 s_0 + \beta_2\beta_1 s_0 - \\ \beta_2\beta_1 v_0 - {\beta_2}^2 v_0 - \theta\beta_1 \end{pmatrix} \tag{44}$$

$$r_2(t) = -\tfrac{1}{2}t^2(\delta\rho i_0 - \mu^2 r_0 + 2\mu\rho i_0 + \rho^2 i_0 - \rho\sigma e_0)$$

Subsequently, further iterations is carried out from the result of (36) which yields at n = 3

$$S_{3c}(t) = -\frac{1}{6}t^3\begin{pmatrix} \mu^3 s_0 + 2\mu\beta_1 s_0 - 2\mu\beta_2 v_0 + {\beta_1}^2 s_0 + \beta_2\beta_1 s_0 - \beta_2\beta_1 v_0 - {\beta_2}^2 v_0 \alpha^2 \mu i_0 s_0 + \\ \alpha^2\beta_1 i_0 s_0 - \alpha^2\beta_2 i_0 v_0 - \alpha^2\theta i_0 + \alpha\delta i_0 s_0 + \ 2\alpha\mu i_0 s_0 + \alpha\rho_0 s_0 + 2\mu\beta_1 s_0 - 2\mu\beta_1 v_0 - {\beta_1}^2 s_0 + \\ 5\beta_2\beta_1 s_0 - \beta_2\beta_1 v_0 - {\beta_2}^2 v_0 - \mu\theta - \theta\beta_1 - \alpha\sigma e_0 s_0 + \alpha\beta_{1_0} s_0 + \mu^2 s_0 + 3\mu\beta_1 s_0 \\ -2\mu\beta_1 v_0 - {\beta_1}^2 s_0 + 4\beta_2\beta_1 s_0 + 2\mu\beta_1 s_0 - 2\mu\beta_1 v_0 - {\beta_1}^2 s_0 + \beta_2\beta_1 s_0 - 5\beta_2\beta_1 v_0 \\ -3{\beta_2}^2 v_0 - \alpha i_0 s_0 - \mu s_0 - 3\beta_1 s_0 + 2\beta_2 v_0 + \theta - \mu\theta - \theta\beta - 2\beta_2\beta_1 v_0 - {\beta_2}^2 v_0 - \\ +2\delta\rho i_0 - \delta\sigma e_0 + \mu^2 i_0 \mu\theta - \theta\beta - 5\beta_1 s_0 - \beta_2 v_0 + \mu v_0 - 3\mu\beta_1 s_0 - 2\mu\beta_2 v_0 + {\beta_1}^2 s_0 \\ +\beta_2\beta_1 s_0 - \beta_2\beta_1 v_0 + 2\alpha\sigma e_0 s_0 + \alpha\sigma_{1_0} s_0 \delta^2 i_0 + 2\delta\mu i_0 + 2\mu\rho {i_0}_1 + 3\alpha\mu i_0 s_0 + \\ \alpha\rho_0 s_0 - 3\alpha\sigma e_0 s_0 + \alpha\sigma_{1_0} s_0 + \alpha\beta_1 i_0 s_0 - \alpha\delta i_0 s_0 + 3\alpha\mu i_0 s_0 + \alpha\rho_0 s_0 - \end{pmatrix}$$

$$S_{3a}(t) = -\frac{1}{6}t^2\begin{pmatrix} \alpha\beta_1 i_0 s_0 - \mu^2 v_0 + 2\mu\beta_1 s_0 - 2\mu\beta_2 v_0 - 2\mu\beta_1 v_0 - {\beta_1}^2 s_0 + \beta_2\beta_1 s_0 - \\ 5\beta_2\beta_1 v_0 - 3{\beta_2}^2 v_0 - \alpha i_0 s_0 - \mu s_0 - 3\beta_1 s_0 + 2\beta_2 v_0 + \theta - \mu\theta - \theta\beta \\ -2\beta_2\beta_1 v_0 - {\beta_2}^2 v_0 - \mu\theta - \theta\beta - 5\beta_1 s_0 - \beta_2 v_0 + \mu v_0 - 3\mu\beta_1 s_0 + \\ {\beta_1}^2 s_0 + \beta_2\beta_1 s_0 - \beta_2\beta_1 v_0 - {\beta_2}^2 v_0 - \theta\beta_1 + \alpha\delta i_0 s_0 + 3\alpha\mu i_0 s_0 + \alpha\rho_0 s_0 \\ -\alpha\sigma e_0 s_0 + \alpha\sigma_{1_0} s_0 + 2\mu\beta_1 s_0 - 2\mu\beta_2 v_0 + {\beta_1}^2 s_0 + 3\beta_2\beta_1 s_0 - \beta_2\beta_1 v_0 \\ -\beta_2 v_0 + \mu v_0 - 3\mu\beta_1 s_0 - 2\mu\beta_2 v_0 + {\beta_1}^2 s_0 + \beta_2\beta_1 s_0 \end{pmatrix}$$

$$e_3(t) = -\frac{1}{6}t^2\begin{pmatrix} \alpha^2 {i_0}^2 s_0 + \alpha\delta i_0 s_0 + 3\alpha\mu i_0 s_0 + \alpha\rho_0 s_0 - \alpha\sigma e_0 s_0 + \alpha\sigma_{1_0} s_0 + \alpha\beta_1 i_0 s_0 + 2\mu\beta_1 s_0 - \\ 2\mu\beta_1 v_0 - {\beta_1}^2 s_0 + 5\beta_2\beta_1 s_0 - \beta_2\beta_1 v_0 - {\beta_2}^2 v_0 - \mu\theta - \alpha\beta_2 i_0 v_0 - 3\alpha\theta i_0 - \\ \mu^2 e_0 - 2\mu\sigma e_0 - \sigma^2 e_0 - \mu^2 r_0 + 2\mu\rho i_0 + \rho^2 i_0 + \alpha\beta_1 i_0 s_0 - 4\alpha\delta i_0 s_0 + 3\alpha\mu i_0 s_0 \\ +\alpha\rho_0 s_0 - 2\alpha\sigma e_0 s + \alpha\delta i_0 s_0 + 3\alpha\mu i_0 s_0 + \alpha\rho_0 s_0 - \alpha\sigma e_0 s_0 + \alpha\sigma_{1_0} s_0 + \alpha\beta_1 i_0 s_0 s_0 \\ -\alpha\beta_2 i_0 v_0 - \alpha\theta i_0 - \mu^2 e_0 - 2\mu\sigma e_0 - \sigma^2 e_0 - \delta\rho i_0 - \mu^2 r_0 - 3\mu\beta_1 - \alpha\beta_2 i_0 v_0 - \\ \alpha\theta i_0 - \mu^2 e_0 - 2\mu\sigma e_0 - \sigma^2 e_0 - \delta\rho i_0 - \mu^2 r_0 - 3\mu\beta_1 + {\beta_1}^2 s_0 + \beta_2\beta_1 s_0 - \beta_2\beta_1 v_0 - \\ {\beta_2}^2 v_0 - \theta\beta_1\alpha\delta i_0 s_0\sigma e_0 - \mu i_0 - \delta i_0 - \rho i_0 + 2\mu\rho i_0 - 2\mu\sigma e_0 + \rho^2 i_0 - \rho\sigma e_0 - \sigma^2 e_0 \end{pmatrix}$$

$$I(t) = -\frac{1}{6}t^2\begin{pmatrix} \alpha\sigma i_0 s_0 + \delta^2 i_0 + 2\delta\mu i_0 + 2\delta\rho i_0 - \delta\sigma e_0 + \mu^2 i_0 + 2\mu\rho i_0 - 2\mu\sigma e_0 - \mu^2 r_0 + \\ 2\mu\rho i_0 + \rho^2 i_0 + \alpha\beta_1 i_0 s_0 - 4\alpha\delta i_0 s_0 + 3\alpha\mu i_0 s_0 + \alpha\rho_0 s_0 - 2\alpha\sigma e_0 s \\ +\alpha\delta i_0 s_0 + 3\alpha\mu i_0 s_0 + \alpha\rho_0 s_0 - \alpha\sigma e_0 s_0 + \alpha\sigma_{1_0} s_0 + \rho^2 i_0 - {\beta_2}^2 v_0 - \mu\theta - \\ \alpha\sigma e_0 s_0 + \alpha\beta_{1_0} s_0 + \mu^2 s_0 + 3\mu\beta_1 s_0 - 2\mu\beta_1 v - \rho\sigma e_0 - \sigma^2 e_0 \\ +2\mu\rho i_0 + \rho^2 i_0 + \alpha\beta_1 i_0 s_0 - 4\alpha\delta i_0 s_0 + 3\alpha\mu i_0 s_0 + \alpha\rho_0 s_0 - 2\alpha\sigma e_0 s + \\ \alpha\delta i_0 s_0 + 3\alpha\mu i_0 s_0 + \alpha\rho_0 s_0 - \alpha\sigma e_0 s_0 + \alpha\sigma_{1_0} s_0 + \alpha\beta_1 i_0 s_0 - \alpha\beta_2 i_0 v_0 \\ -\alpha\theta i_0 - \mu^2 e_0 - 2\mu\sigma e_0 - \sigma^2 e_0 - \delta\rho i_0 \end{pmatrix}$$

$$r_2(t) = -\frac{1}{6}t^2\begin{pmatrix} \delta\rho i_0 - \mu^2 r_0 + 2\mu\rho i_0 + \rho^2 i_0 + \sigma^2 e_0 - \mu^2 r_0 + 2\mu\rho i_0 + \rho^2 i_0 + \alpha\beta_1 i_0 s_0 \\ -4\alpha\delta i_0 s_0 + 3\alpha\mu i_0 s_0 + \alpha\rho_0 s_0 - 2\alpha\sigma e_0 s + \alpha\delta i_0 s_0 + 3\alpha\mu i_0 s_0 + \alpha\rho_0 s_0 \\ -\alpha\sigma e_0 s_0 + \alpha\sigma_{1_0} s_0 + \alpha\beta_1 i_0 s - \rho\sigma^2 e_0 \end{pmatrix}$$

This can be furthered till the desired number of iterations are obtained. Hence, the summary of iterative solutions to each model compartment is obtained as;

$$S_c(t) = \sum_{k=0}^{3} s_k(t), S_a(t) = \sum_{k=0}^{3} v_k(t), E(t) = \sum_{k=0}^{3} e_k(t), I(t) = \sum_{k=0}^{3} i_k(t), R(t) = \sum_{k=0}^{3} r_k(t), \quad (45)$$

And evaluating these results using the corresponding model parameters of each class given by

$$\left.\begin{array}{c} \alpha = 0.008, \delta = 0.4, \mu = 1.0, m = 0.1, \sigma = 0.9, \pi = 2.19, \gamma_1 = 1.263, \kappa = 0.002, \\ \gamma_e = 0.03, \varphi_1 = 1.82, \gamma_e = 0.03, \varphi_1 = 1.82, \\ v = 0.5, \phi = 0.2, \varphi_2 = 0.002, \beta = 1.0003, e_0 = 653930, s_{0c} = 500000, \\ s_{0a} = 26000, i_0 = 23890, r_0 = 14730 \end{array}\right\}$$ It is therefore obtained that;

$$S_c(t) = 500 - 30.4320t + 0.7213561075t^2 - 0.03863404097t^3$$

$$S_a(t) = 120 - 1.5060t - 0.01591470000t^2 + 0.00061794336453t^3$$

$$E(t) = 65 + 18.1785t - 1.171778775t^2 + 0.04155466537t^3 \quad (46)$$

$$I(t) = 23 - 0.9060t + 0.02925067500t^2 - 0.0008440367800t^3$$

$$R(t) = 14 - 0.0155t - 0.005054500000t^2 + 0.0001458242542t^3$$

The approximate results of each class are evaluated using their respective baseline values in obtained from table 2. We also suggest the following population data set as initial values given by

$s_{0c} = 500000, s_{0a} = 26000, e_0 = 653930, i_0 = 23890, r_0 = 14730$. Thus we obtain the following series of results embedding the parameters whose influence on the dynamics of measles transmission are to be analysed as:

$$S_c(t) = 1000 + \begin{pmatrix} 273.20 + 1.383730\sigma \\ -1.6353\sigma^2 - 37.68m \end{pmatrix} t + \begin{pmatrix} -4672.\sigma^2 \\ +29.8635\sigma^4 \\ 54.0914019 \\ +1.5361\alpha^2 c \end{pmatrix} \frac{t^2}{2} - \begin{pmatrix} 0.652^2 c^2 \\ -0.5242\alpha^3 \\ -0.83736\sigma\varphi^2 \\ +2.9365\alpha^4 \\ +935.98111186\alpha^2 c \\ +56.12092345c \\ -5.923814565\alpha \\ 10.352 \\ +635.09\sigma^6 \\ -1.86344\sigma \end{pmatrix} \frac{t^3}{6}$$

$$S_a(t) = 1000 + \begin{pmatrix} 65.26869000 + 1.3362000\alpha \\ -1362.924000\alpha^2 - 37.68c \end{pmatrix} t + \begin{pmatrix} -8.99856418\alpha^2 \\ +152.0510083\alpha^2 c \\ -0.09970881600\alpha c \\ +3333.926349 \\ 45.98509816c \\ -3.288025569\alpha \end{pmatrix} \frac{t^2}{2} - \begin{pmatrix} 11.30828286\alpha^2 c^2 \\ -66.76103861\alpha^3 \\ -0.003719829888\alpha c^2 \\ +40645.08576\alpha^4 \\ +935.98111186\alpha^2 c \\ -84.74264814\alpha \end{pmatrix} \frac{t^3}{6}$$

$$E(t) = 30 + \begin{pmatrix} -45.62599000 \\ +1362.924999\alpha^2 \\ -1.336200000\alpha \end{pmatrix} t - \begin{pmatrix} -69.38980854c \\ -0.09970881600\alpha c \\ +5378.993811\alpha^2 \\ +0.0000493608c \\ -5.292993669\alpha \end{pmatrix} \frac{t^2}{2} + \begin{pmatrix} 11.30828286\alpha^{2^2} - 80.26339203\alpha^3 \\ -0.7679873978\alpha c + 1431.639314\alpha^4 c \\ -1.875838588\alpha^3 c + 16753.17626\alpha^2 \\ +0.0003841080404c - 16.31203298\alpha \\ +36988.74452\alpha^6 - 84.74264814\alpha^5 \end{pmatrix} \frac{t^3}{6}$$

$$I(t) = 17 - 0.6373t - \begin{pmatrix} 127.0391180 \\ +0.63524\phi^2 \\ -0.7283\phi \end{pmatrix} \frac{t^2}{2} - \begin{pmatrix} -0.004499284709\alpha^3 \\ +320.2194878 \\ -0.00004985440800\alpha c \\ +4.407401276\phi^2 \\ +2.46825 \cdot 10^{-8} d \\ -0.004339725d \end{pmatrix} \frac{t^3}{6} \quad (47)$$

$$R(t) = 40 + (46.18360 + 37.68c)t - \begin{pmatrix} 250.8099123 \\ +45.9850488c \\ -2044.386000\phi^2 \end{pmatrix}\frac{t^2}{2} + \begin{pmatrix} 13.49785413\alpha^3 \\ -8249.759899\alpha^4 \\ +727.7734324 \\ +56.12053936d \\ +10.38388802\phi \end{pmatrix}\frac{t^3}{6}$$

Results and discussion

The interpretation of numerical simulation conducted through iterative steps of homotopy perturbation method is depicted diagrammatically below.

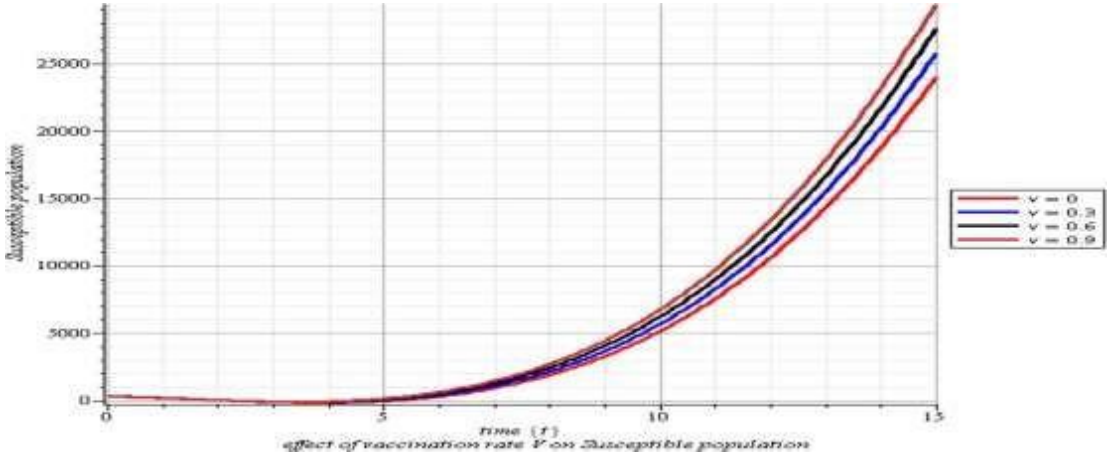

Figure 2. Effect of Vaccination Rate v on Susceptible Population

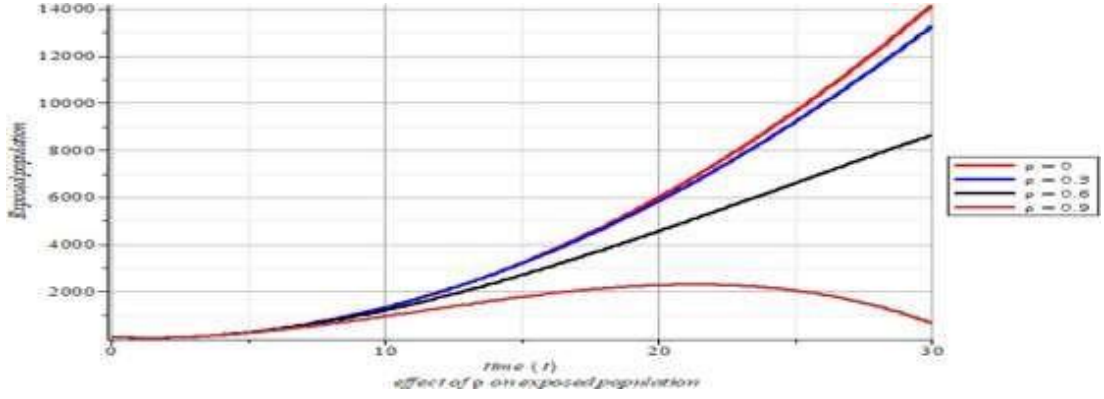

Figure 3. Effect of vaccination rate v on exposed population

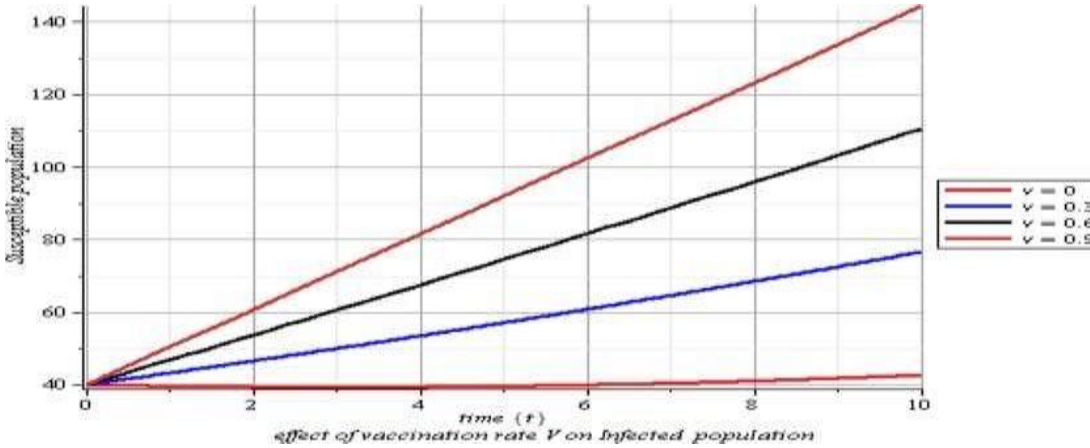

Figure 4. Effect of vaccination rate v on Infected Population

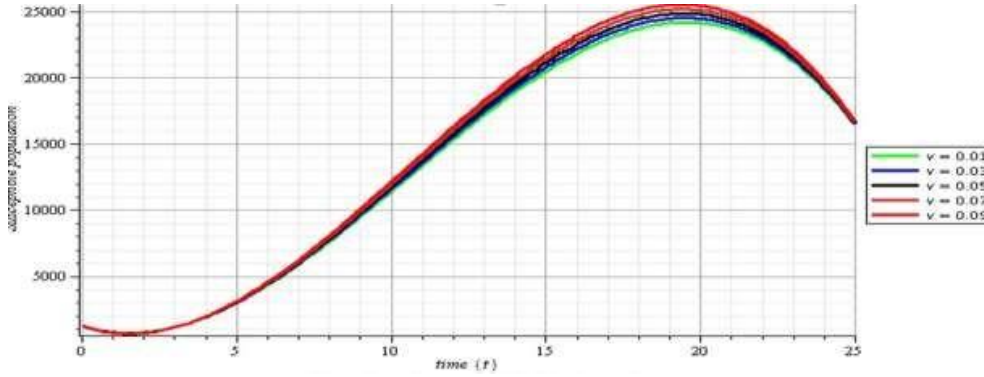

Figure 5. Effect of vaccination rate ω on infected population

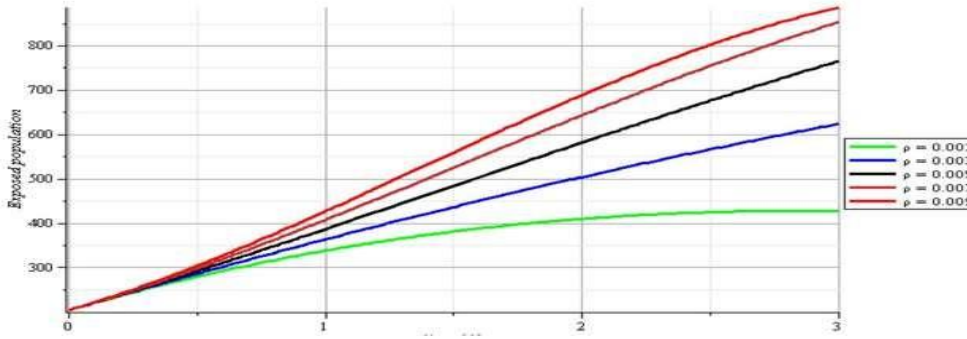

Figure 6. Effect of vaccination rate ω on susceptible population

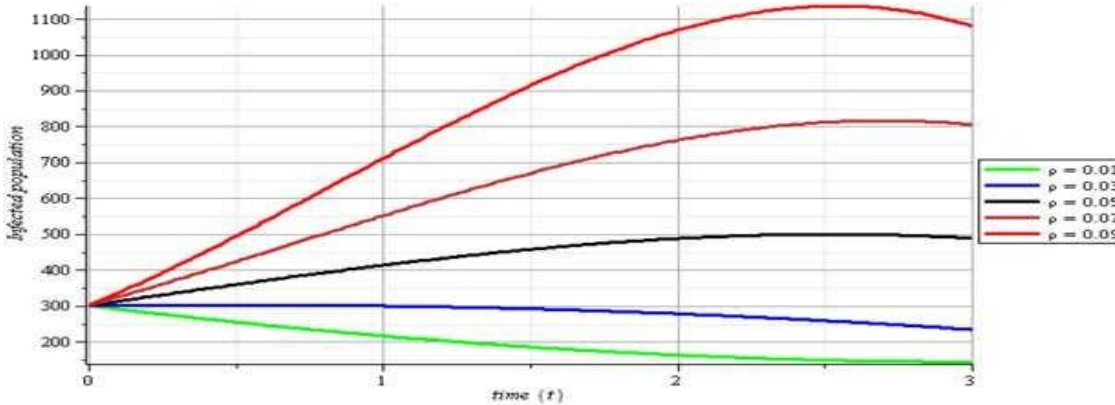

Figure 7. Effect of vaccination rate ω on exposed population

In this graphical illustration, maple 18 software was utilized to simulate the disease dynamics over time with respective compartments. The findings are presented in a graphical format and extensively discussed. Fig.2 illustrates that as the vaccination rate increases, the vulnerable population also increases. Meanwhile, Fig.3 demonstrates that when the vaccination rate goes from 0.0 to 0.9, the exposed population decreases. This suggests that an increase in vaccination rates results in a higher number of susceptible individuals and a decrease in vaccination rates leads to a higher number of exposed individuals. Additionally, as the vaccination rate rises, the exposed population decreases, as observed in Fig.4. over 20 months, it was noted that as the vaccination rate increases from 0.03 to 0.09, the infected population decreases. Fig.5 reveals that an increase in vaccination results in a reduction in the number of infected individuals, consequently increasing the population of susceptible individuals while fig.6 highlights the impact of vaccination on the susceptible population, particularly after recovery. Through treatment, susceptible individuals can be effectively recovered from the disease. In this context, vaccinating those who have recovered can significantly reduce the prevalence of the disease in the population and fig.6 explores the effects of the waning rate on exposed individuals. An increase in the waning rate leads to a reduction in the population of exposed individuals. For instance, when the waning rate is 0.01, more individuals are less likely to become infected, resulting in an increased population of susceptible individuals.

Conversely, reducing the waning rate increases the infected population.

Conclusion

This paper has been able to utilize the homotopy perturbation method to derive a numerical solution for the impact of high treatment vaccination efficacy on a measles model of SVEIR. This approach proved highly effective in yielding accurate model results bring the basic threshold of measles spread to less than unity. Subsequently, numerical output was simulated to assess the influence of vaccination saturation on measles transmission within the population, with careful analysis of the accompanying graphs to reveal key experimental and biological impact on the sub-populations with time. Nevertheless, it is important to note that further research is essential to address the ongoing prevalence of this epidemic disease and to develop effective strategies for its containment and eradication and vaccination and treatment rate will suffice for certain period of combat towards the spread of measles. The promotion of awareness, educational programs as preventive measures is crucial to policy makers and practitioners of health in controlling of the spread of measles in the future.

Declaration of Competing Interest

The authors of the paper declared that there are no conflicts of interest.

Acknowledgment

The authors acknowledge the tremendous efforts of the anonymous reviewers of this manuscript.

Conflict of interest

The authors do not have a conflict of interest in the publication of this paper.

Data Availability Statement

Data sets generated during the current study are available from the corresponding author upon reasonable request.

Authorship Contribution Statement

- Saheed A. BELLO: Data preparation, analysis, reviewing
- Kazeem A. ODEYEMI: Supervision, analysis, simulation, Conceptualization, methodology
- Olumide O OLAIYA: Methodology, computation, qualitative analysis.
- Victor A. AKINRINMADE: Simulation, analysis, Typesetting

References

Agusto, F. and Leite, M. (2019). "Optimal control and cost-effective analysis of the 2017 meningitis outbreak in Nigeria," Infectious Disease Modelling, vol. 4, pp. 161–187.

Asamoah, J. K. K. Nyabadza, F. Seidu, B. Chand, M. and Dutta, H. (2018). "Mathematical modeling of bacterial meningitis transmission dynamics with control measures," Computational and Mathematical Methods in Medicine, Article ID 2657461, 21 pages,

Ayoola T, Kolawole M, Popoola A (2022), "Mathematical Model of COVID-19 Transmission Dynamics with Double Dose Vaccination". https://www.ajol.info/index.php/tjs

Ayoola TA, Kolawole MK, Popoola AO. (2022). Mathematical model of COVID-19 transmission dynamics with double dose vaccination. Tanzan J Sci 48(2):499–512. https:// doi. org/ 10. 4314/ tjs. v48i2. 23

Bhandari, M., Rathnayake, I. U., Huygens, F., Nguyen, S., Heron, B., & Jennison, A.V. (2023). Genomic and Evolutionary Insights into Australian Toxigenic Vibrio cholerae O1 Strains. *Microbiology Spectrum*, *11*(1). https://doi.org/10.1128/

Bozkurt F., Ali Y., Abdeljawad T., Adem K., Al Mdallal Q. (2021) A fractional order model of COVID-19 considering the fear effect of the media and social networks on the community. Chaos Solitons Fractals 152:111403

Castillo, C., Feng, Z., and Huang, W. (2002). "On the computation of 0 R and its role in global

stability in mathematical approaches for emerging and reemerging infectious diseases": An Introduction Springer, 125: 229– 250

Castillo, C., Feng, Z., and Huang, W. (2018). "On the computation of basic reproduction number and its role in global stability in mathematical approaches for emerging and reemerging infectious diseases": An Introduction Springer, Vol. 125, 2002, pp.229– 250

Dejongh, F. (2021). "New global meningitis strategy aims to save 200,000 lives a year," 2021, https://news.un.org/en/story/ 2021/09/1101352

Ferguson EA, Brum E, Chowdhury A, Chowdhury S, Kundegorski M, Mahmud AS, Purno N, Sania A, Steenson R, Tasneem M, Hampson K (2022) Modelling how face masks and symptoms-based quarantine synergistically and cost-effectively reduce SARS-CoV-2 transmission in Bangladesh. Epidemics 40:100592. https:// doi. org/ 10. 1016/j. epidem. 2022. 100592

Kolawole, A. I., Alaje, M. O. Ogunniran, and K. R. Tijani, "Simulating the effect of disease M. K. transmission coefficient on a disease induced death series epidemic model using the homotopy perturbation method," Journal of Applied Computer Science & Mathematics, vol. 16, no. 33, 2022.

Kolawole, M.K., Ayoola, T.A. and Abdulrasaq, R. "Modelling typhoid fever with general knowledge, vaccination and treatment for susceptible individual". International Journal of Research and Innovation in Applied Science, vol. 5, no. 3, 2020, pp. 2454-2469.

Kolawole, M.K., Ogundeji, O.D. and Popoola, A.O. (2020). "Comparison of saturation term and disease induced in SIR epidemic model", International Journal of Research and Innovation in Applied Science, vol. 5, No. 1, pp. 24546194.

Kolawole, M.K., Olayiwola, M.O. and Odeyemi, K. A., (2023). "Conceptual analysis of the combined effects of vaccination, therapeutic actions, and human subjection to physical constraint in reducing theprevalence of COVID-19 using the homotopy perturbation method". Beni-SuefUniversity Journal of Basic Applied and Science, 12(10), https://doi.org/10.1186/ s43088-023-00343-

Mojtaba, I. M. EL and Adam, S. O. (2017). "A mathematical model for meningitis disease," Red Sea University Journal of Basic and Applied Science, 2: 467–472.

Mutairu K. Kolawole, Bukola. O. Akin-awoniran, K., Odeyemi, A. (2023). On the Numerical Analysis of the Effect of Vaccine on Measles using Virational Iteration Method. Jurnal diferensial. 5(2) DOI: https://doi.org/10.35508/jd.v5i2.

Mutairu k. Kolawole, Kazeem, A. Odeyemi, Kehinde A. Bashiru, Popoola, A.O. (2023). An Approximate Solution of Fractional Order Epidemic Model of Typhoid using Homotopy Perturbation Method. UNIOSUN Journal of Engineering and Environmental Sciences, Vol. 5 No. 1. DOI: 10.36108/ujees/3202.50.0180.

Mutairu K. Kolawole, Morufu O. Olayiwola, Kazeem, A. Odeyemi, Adedapo I. Alaje, (2023) Extensive Analysis and Projection of the Impact of High-Risk Immunity Using a Mathematical Model That Incorporate a Convex Incidence Rate of Multiple Covid-19 Exposures. Cankaya University Journal Science and Engineering. CUJSE 20(02): 107-128.

Mutairu K. Kolawole, Muideen O. Ogunniran, Kazeem, A. Odeyemi (2023) On the Numerical Simulation of the Effect of Disease Transmission Coefficient on SEIR Epidemic Model Using Hybrid Block Method. Jurnal diferensial. Issue 2, Vol 5 No. 2. OI: https://doi.org/ 10.35508/jd.v5i2. Indonesia

Mutairu k. Kolawole, Oluwarotimi O. Aderonke, Kazeem, A. Odeyemi, Amos O. Popoola (2023) Analysis of Corona-Virus Mathematical Model in Asymptotic and Symptomatic Cases with Vaccine using Homotopy Perturbation Method. Journal of Applied Computer Science & Mathematics, Issue 1, vol.17, No. 35, Suceava.

Mutairu K., Kolawole, K., Adedapo, A., Alaje, O., Asimiyu, I., Oladapo, O. and Bashiru, K.A. (2022). Dynamical Analysis and

Control Strategies for Capturing the Spread of Covid-19. Tanzania Journal of Science 48(3): 680-690.

Opoku, N. K.-D. O. and Afriyie, C. (2020). "The role of control measures and the environment in the transmission dynamics of cholera," Abstract and Applied Analysis, vol. 2020, Article ID 2485979, 16 pages, 2020. spectrum.03617-22

WHO (World Health Organization) .(2020). Emergencies, preparedness, response. Pneumonia of unknown origin-China, Disease Outbreak News. 5. https:// www. who. int/ csr/ don/ 05- janua ry- 2020- pneum onia- of- unkow ncause- china/ en/. Accessed 5 Mar 2020

Wusu AS, Olabanjo MA and Akanbi J. (2022). A model for analyzing the dynamics of the second wave of coronavirus (COVID-19) in Nigeria. J. Math. Comput. Sci. 26: 1621.